Numerical Simulations to support Alaska Production Testing

Evgeniy Myshakin
NETL Support Contactor

U.S. Department of Energy
National Energy Technology Laboratory
Resource Sustainability Project Review Meeting
April 2-4, 2024

Project Overview

Project Goals:

- Provide the state-of-the-art experimental, modeling, and economic analysis to support planning and execution of long-term field gas production tests, predicting environmental implications and developing long-term projection of US energy asset.
- Provide pertinent, high-quality information that benefit the development of geological and numerical models and methods for predicting the behavior of gas hydrates in natural and production conditions.

Overall Project Performance Dates: 04/01/2023 – 03/31/2024

Project Participants:

- FE HQ Division Director; Vanessa Nunez-Lopez
- FE HQ Project Manager: Sailendra Mahapatra
- NETL Technology Manager: John Rogers
- NETL Senior Fellow: Ale Hakala
- NETL Program Manager: Erich Zorn
- NETL R&IC TPL: Yongkoo Seol
- NETL R&IC Researchers
- LRST Site Support Researchers
- ORISE Fellows
- Universities: West Virginia Univ., RPI, Georgia Tech,TAMU

Location of the Kuparuk 7-11-12 Pad and Drilled wells

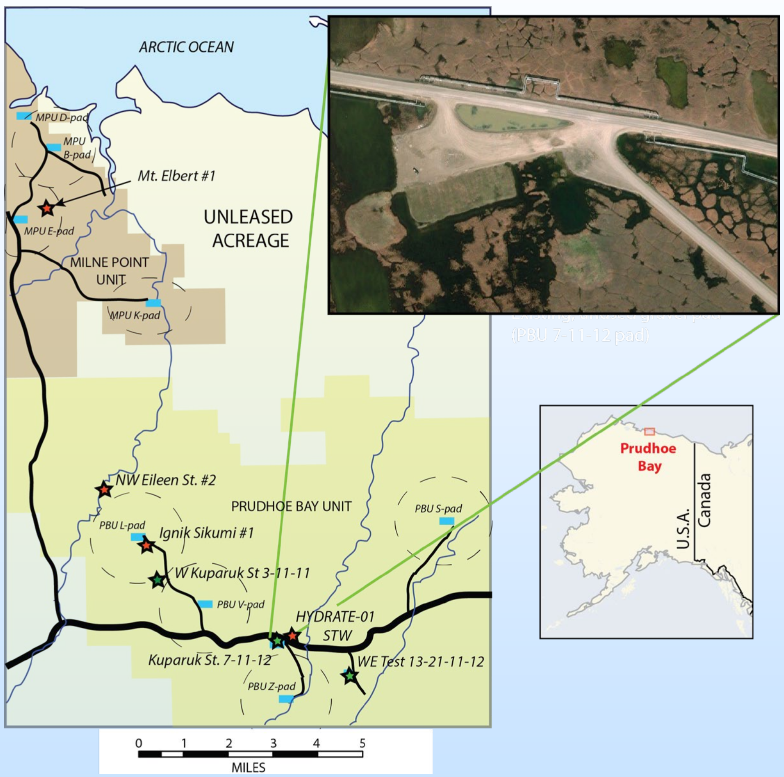

The locations of gas hydrate research projects are designated by red stars. Inset shows the existing 7-11-12 gravel pad from which two exploratory wells were drilled. This pad was selected as the surface location for the Hydrate-01 well drilled in December 2018.

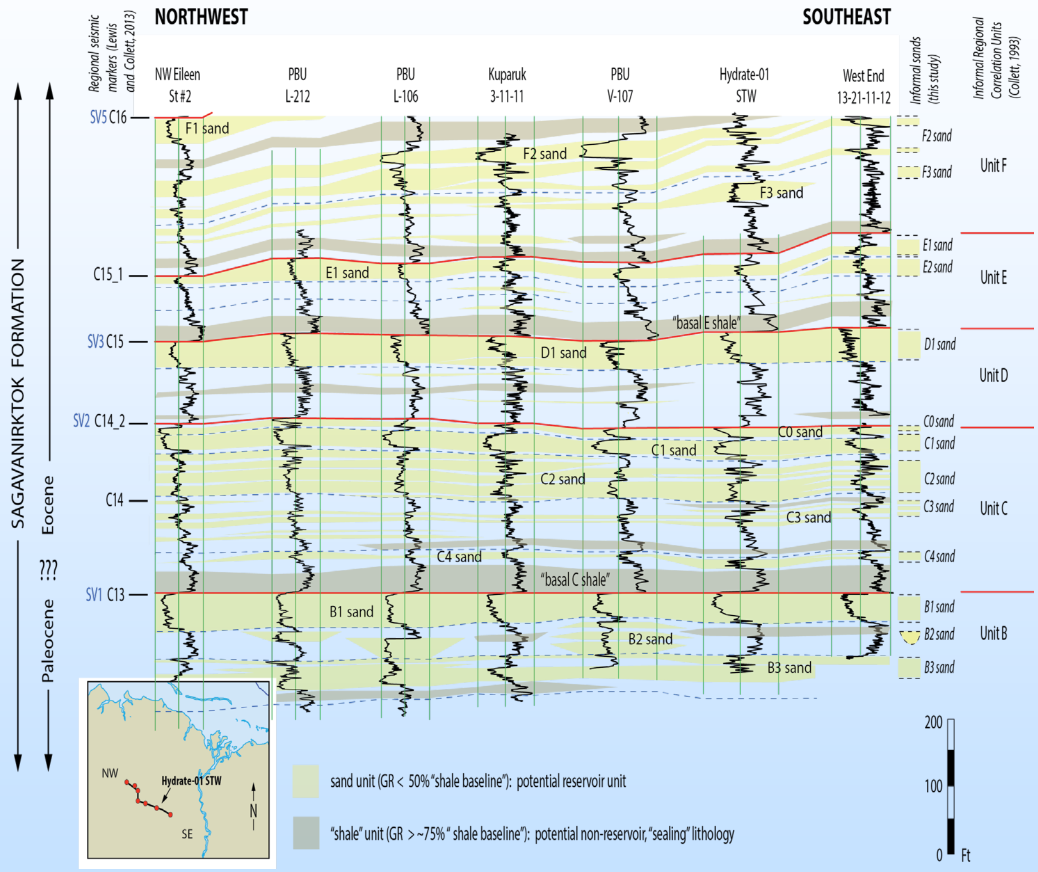

Gamma-ray well log cross-sections of geologic units (Units B, C, D, E, and F) that commonly contain gas hydrate in the western Prudhoe Bay Unit, Alaska North Slope

Boswell et al., 2022

The gas hydrate reservoir characterization at the BPU Kuparuk 7-11-12 Pad on Alaska North Slope

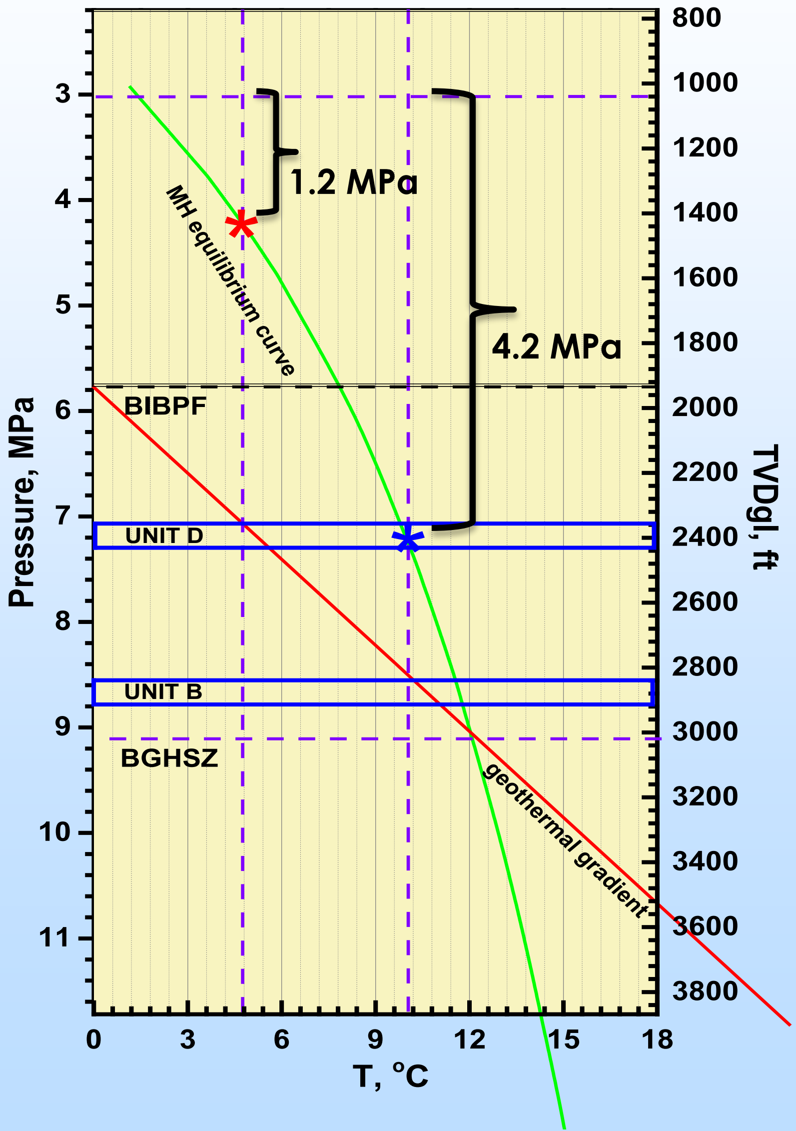

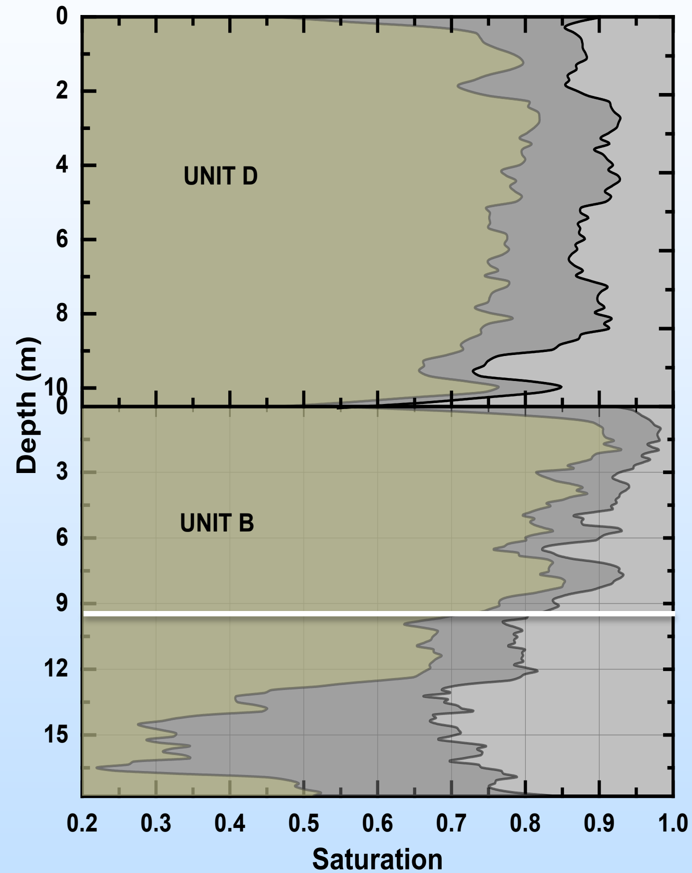

Gas hydrate (yellow), irreducible (gray) and free (light gray) water saturations in Units D and B.

Two-dimensional reservoir models of the gas hydrate reservoirs at the Kuparuk site

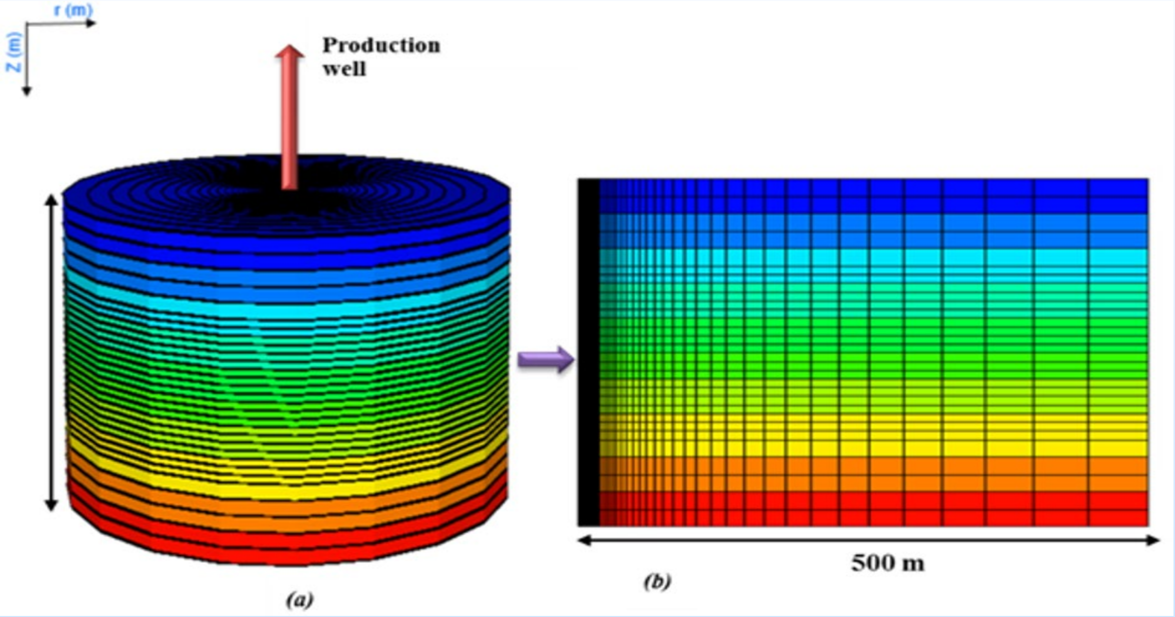

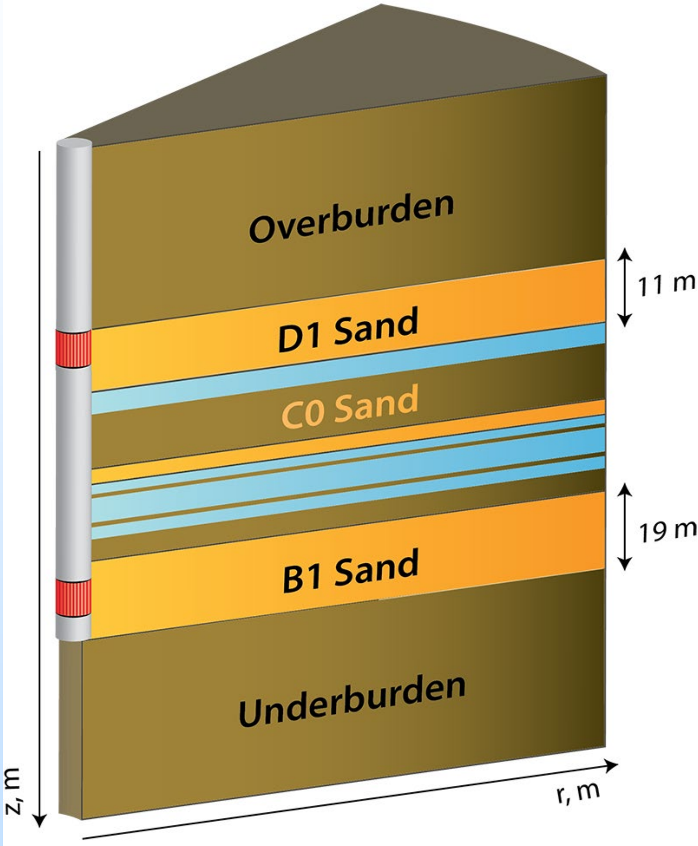

- Two models with lateral extensions of 500 and 3,000 m
- Logarithmic distribution of mesh elements in the lateral direction.
- In reservoir units, vertical discretization is 0.10 m per layer.
- Mesh contains 86,052 elements and 171,476 connections (for a model with a 500-m radius).
- Heterogenous property distributions with depth based on Logging-While-Drilling and core data.

Input technical parameters and equation used in the simulations

	Equations and parameters	Comments
Relative permeability and capillary pressure functions	Permeability adjustment due to gas hydrate presence: $k_{adj} = k_{int}(1 - S_{gh})^N$ The Brooks-Corey equation for relative permeability: $k_{r(w,g)} = k_{r(w,g)co}\left(\frac{1-S^*_{(g,w)}-S^*_{(g,w)ir}}{1-S^*_{wir}-S^*_{gir}}\right)^{n(w,g)}$ $S^*_{(w,g)} = \frac{S_{(w,g)}}{1-S_{gh}}$; $nw = 6.7$; $ng = 1.6$; $k_{rw\_gco}=1.0$; and $k_{rg\_wco}=0.377$, $S^*_{gir} = S_{gir} = 0$ The van Genuchten function for capillary pressure: $P_{cap} = -P_{c0}\left[(S^c_w)^{-1/\lambda} - 1\right]^{1-\lambda}$; $S^c_w = \frac{(S_w - S_{wir})}{(1-S_{wir})}$ $\lambda=0.77437$; $P_{c0} = 909$ Pa	
Thermal conductivity [W/mK]	Composite thermal conductivity (k_θ, the liner model by Bejan): $k_\theta = (1-\phi)k_{\theta\,matrix} + \phi\left(S_g k_g + S_w k_w + S_{gh} k_{gh} + S_I k_I\right)$ where S_g, S_w, S_{gh}, and S_I are gas, aqueous, gas hydrate, and ice saturations, respectively, multiplied by the corresponding thermal conductivities below: .	
Pore compressibility, [Pa^{-1}]	10^{-9} (averaged) and 10^{-10} (averaged) for reservoir and non-reservoir sections, respectively. The estimates are based on interpretation on sidewall pressurized core sample measurements.	
Grain specific heat, *Cp* [J/kg/K]	800	The estimate is based on the specific heat measurement.
Salinity, ppt	5	
Rock density, kg/m^3	2,650	The estimate is based on averaging over core measurements.
Salinity effect on the equilibrium curve	The simplified Dickens and Quinby-Hunt model is used $\Delta T_{NaCl} = \Delta T_{NaCl,r}\frac{\ln(1-X_{NaCl})}{\ln(1-X_{NaCl,r})}$ where ΔT_{NaCl} is inhibitor-induced temperature depression [K] at and X_{NaCl}, mole fraction of the inhibitor in aqueous phase; $\Delta T_{NaCl,r}$ and $X_{NaCl,r}$ are reference temperature depssion and mole fraction, respectively.	
Methane dissolution in water	Henry's law: $P^m_G = H^m(T)X^m_A$ where P^m_G is methane partial pressure in gas phase; $H^m(T)$ is temperature-dependent Henry's coefficient; X^m_A is mole fraction of methane dissolved in aqeous phase.	

Modeled depressurization scenarios and perforated well interval

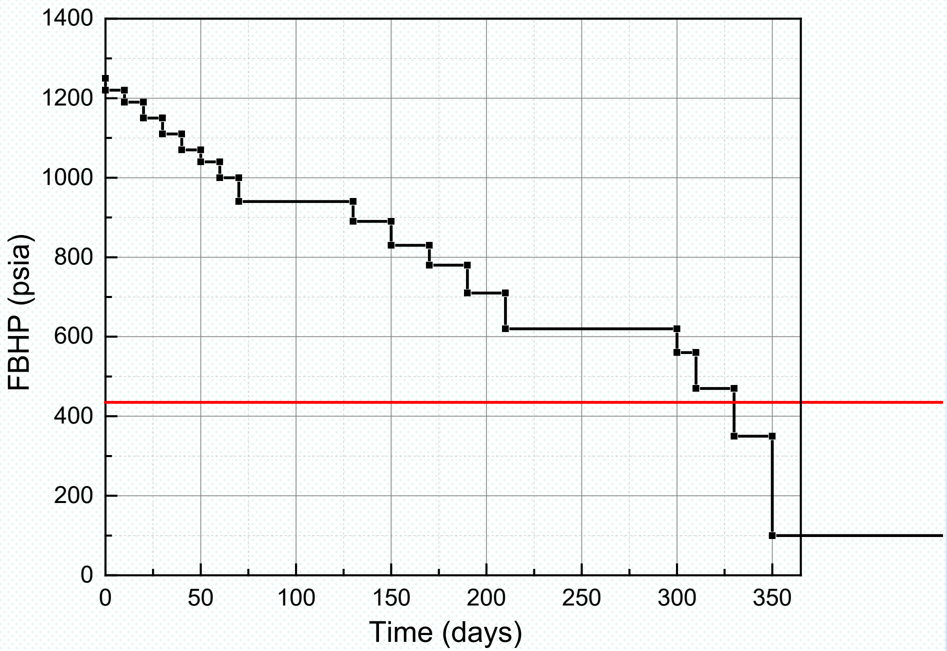

- **Scenario 1: Depressurization at a constant bottomhole pressure (BHP), 3.0 MPa.**
- **Scenario 2: Depressurization with a flowing bottomhole pressure (FBHP) to keep water rate at a prescribed level.**
- **Scenario 3: 16 stages of step-wise decrease for FBHP; from 1250 psia (8.62 MPa) to 350 psia (2.41 MPa) at day 365.**
  First 30 days no gas hydrate dissociation induced: flow assurance.

Gas hydrate reservoir in B1 sand:
All scenarios: the perforated interval was 7.0 m and located 3.0 m below the top boundary.
Scenario 2: the interval was also shifted up to the top boundary.

Gas hydrate reservoir in D1 sand:
Scenario 1: the perforated interval was 5.5 m and set at the top boundary

Comparison of modeled productivity between gas hydrate reservoirs in Unit D and Unit B

GAS PRODUCTION

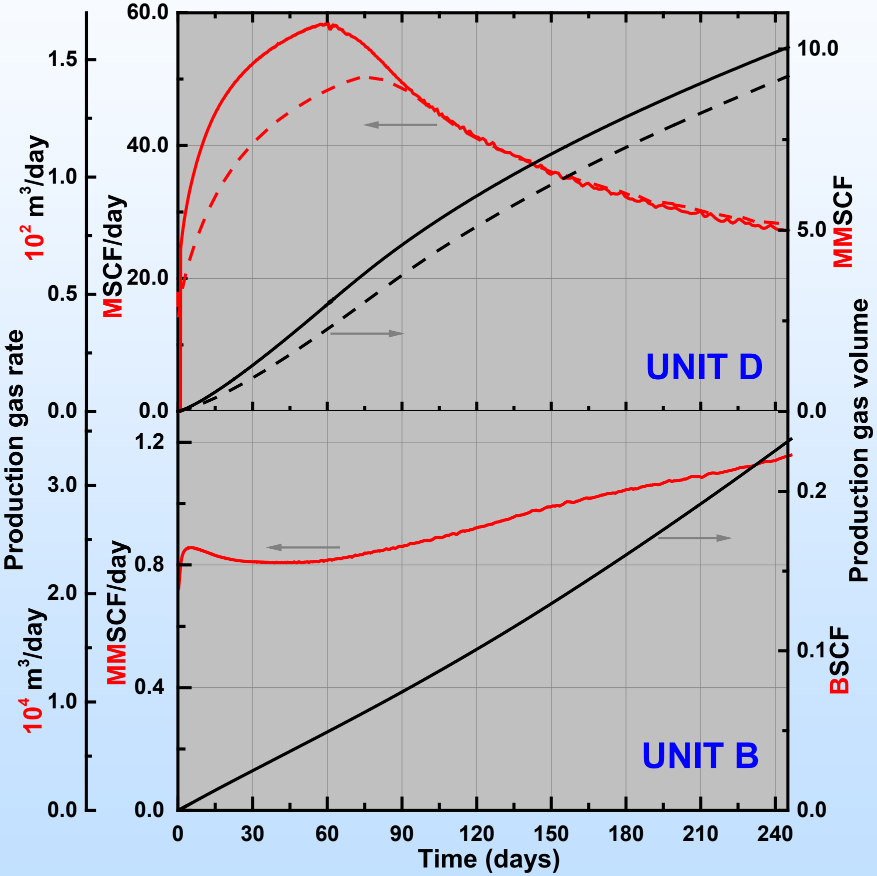

WATER PRODUCTION

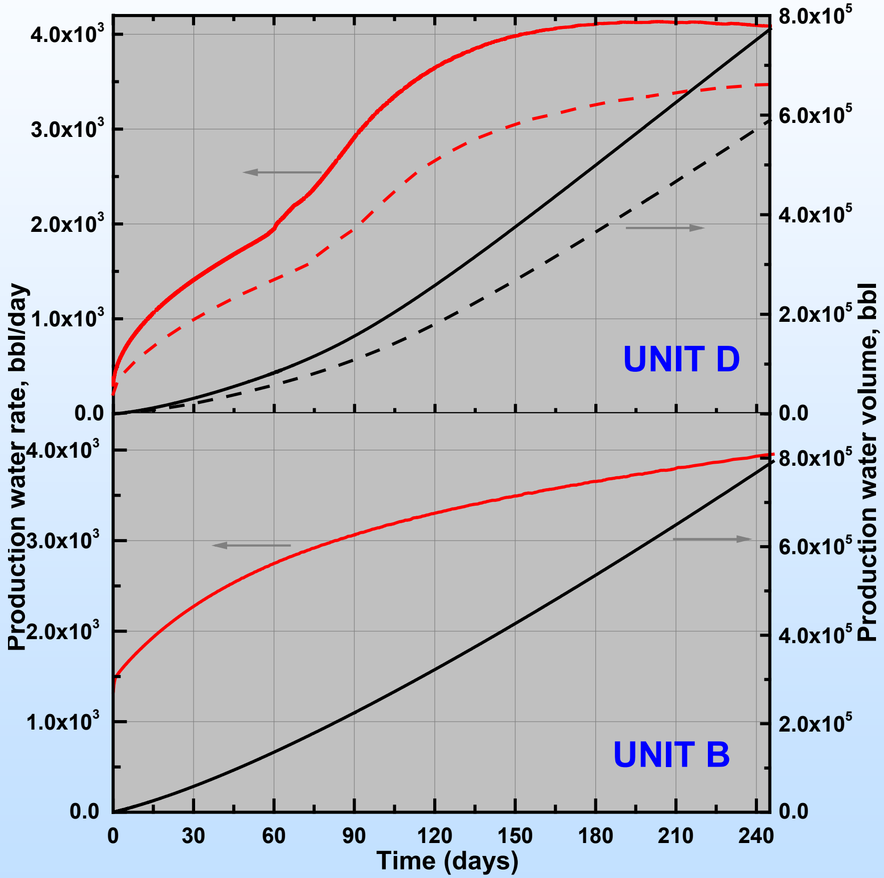

- Temperature: 4.73 °C (Unit D) and 10.03 °C (Unit B)
- Depressurization @ 3.0 MPa BHP (Scenario 1)
- Pressure driving force: 1.20 MPa (Unit D) and 4.20 MPa (Unit B)

Comparison of pressure distribution in D1 sand

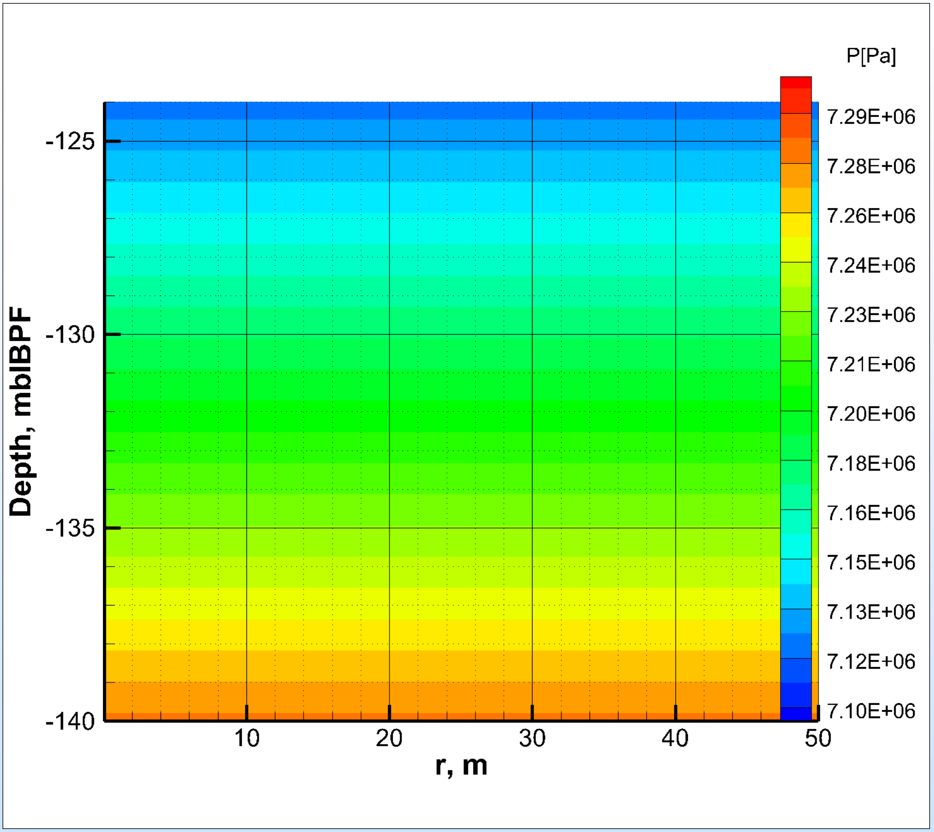

Initial distribution

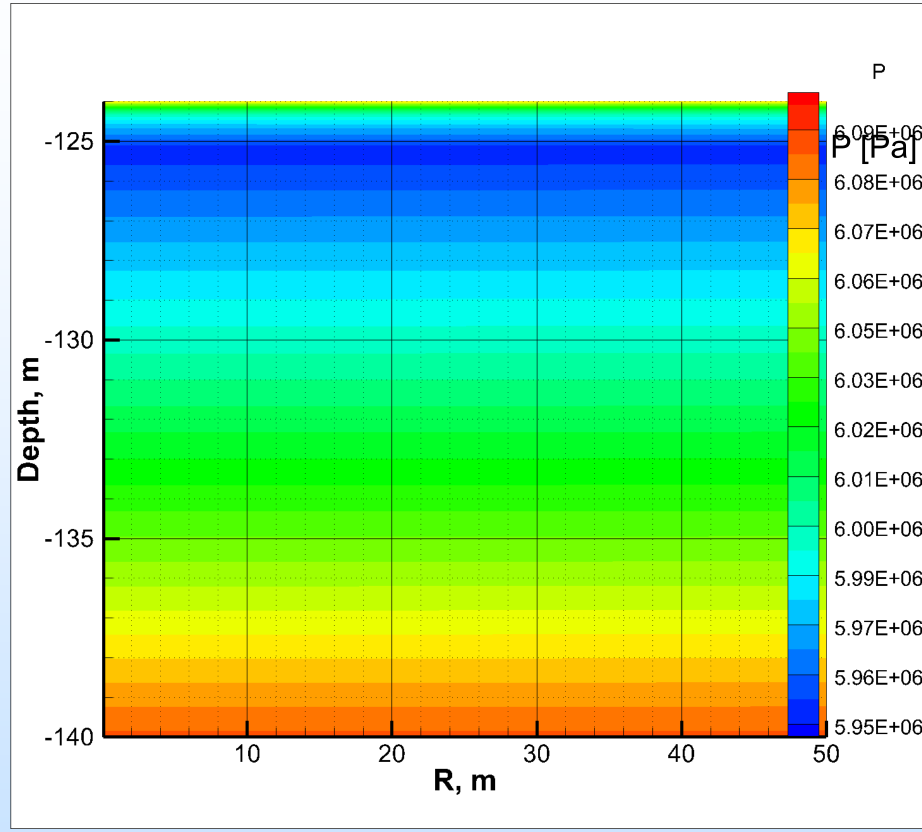

After 1 year of depressurization (3.0 MPa) in B1 sand

- The bottom of the D1 sand and the top of the B1 sand are separated by 436 ft.
- On average the pressure in the D1 sand dropped by about 1.2 MPa after 1 year of depressurization in the B1 sand (Scenario 1).

Water Rate Control with Variable BHP

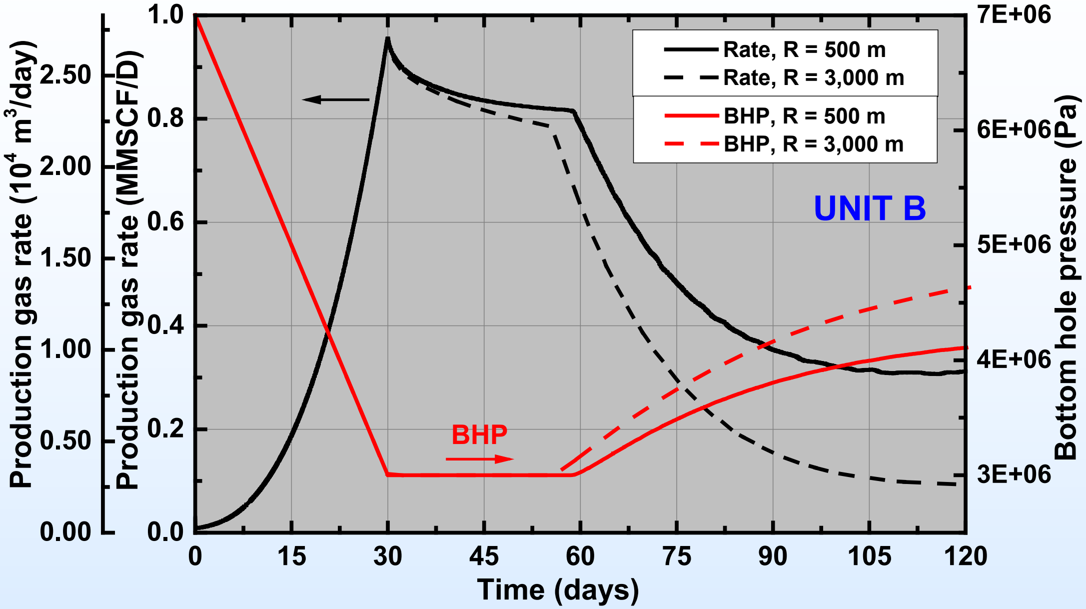

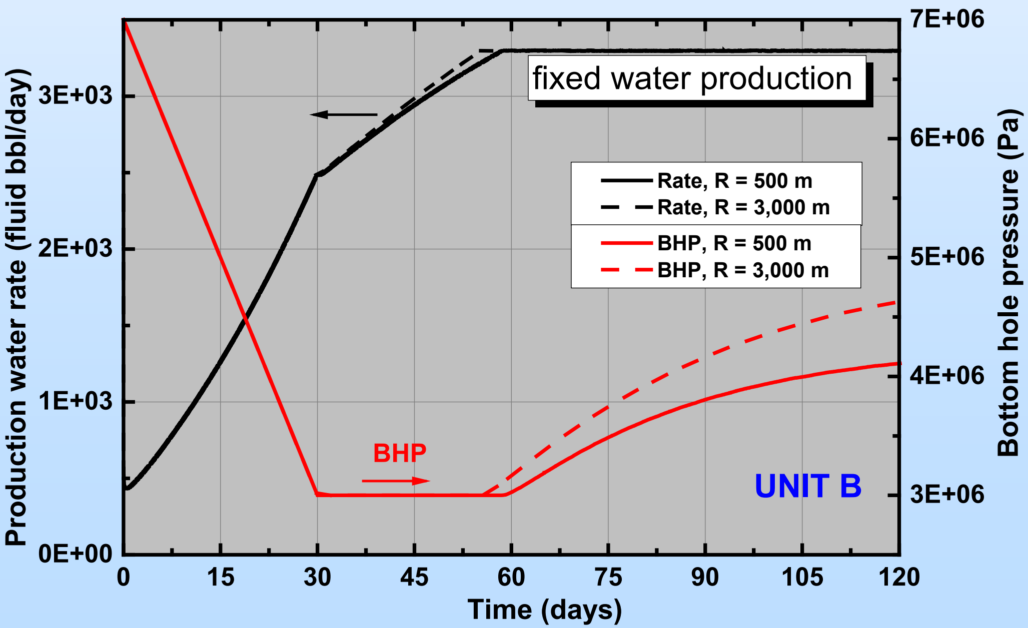

- ✓ Scenario 2 used
- ✓ To maintain the prescribed water rate, FBHP has to be gradually increased from 3.0 MPa.
- ✓ Gas rate decreases from 0.8 MMSCF/day to 0.3 and 0.1 MMSCF/day for the models with 500 and 3,000 m radii, respectively.

Sensitivity analysis of production cases

CASE C	BASE CASE
CASE 1	CASE C with a 7-m production interval shifted to the top boundary
CASE 2	**CASE 1** with sharp permeability contrast at the top boundary
CASE 3	**CASE 1** with a 1:10 anisotropy ratio for non-reservoir units (Case C uses 1:5)
CASE 4	**CASE 1** with anisotropy and "sharp contrast" (**CASE 2** + **CASE 3**)

Geological input at the boundary between B1 sand and overburden

MD, ft	TVDss, ft	Unit	porosity	Sh	Keff, md	Kint, md	Keff, md	Kint, md
					CASES C, 1, and 3		CASES 2 and 4	
3000.0	2768.17	overburden	0.271	0.000	2.27	2.27	1.0	1.00
3000.5	2768.64	overburden	0.305	0.000	2.67	2.67	1.0	1.00
3001.0	2769.11	Upper B1 sand	0.333	0.538	26.42	198.54	8.0	2500.00
3001.5	2769.58	Upper B1 sand	0.367	0.648	29.50	451.55	8.0	2500.00
3002.0	2770.05	Upper B1 sand	0.391	0.740	27.71	894.19	8.0	2500.00
3002.5	2770.51	Upper B1 sand	0.407	0.805	20.74	1315.15	8.0	2500.00
3003.0	2770.98	Upper B1 sand	0.422	0.860	14.50	1900.28	8.0	2500.00

Reservoir performance using sensitivity cases

GAS PRODUCTION

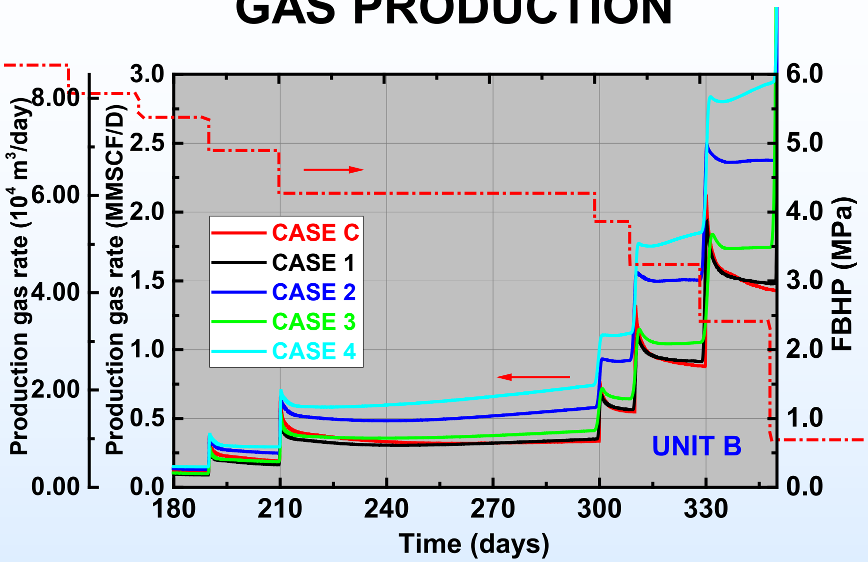

WATER PRODUCTION

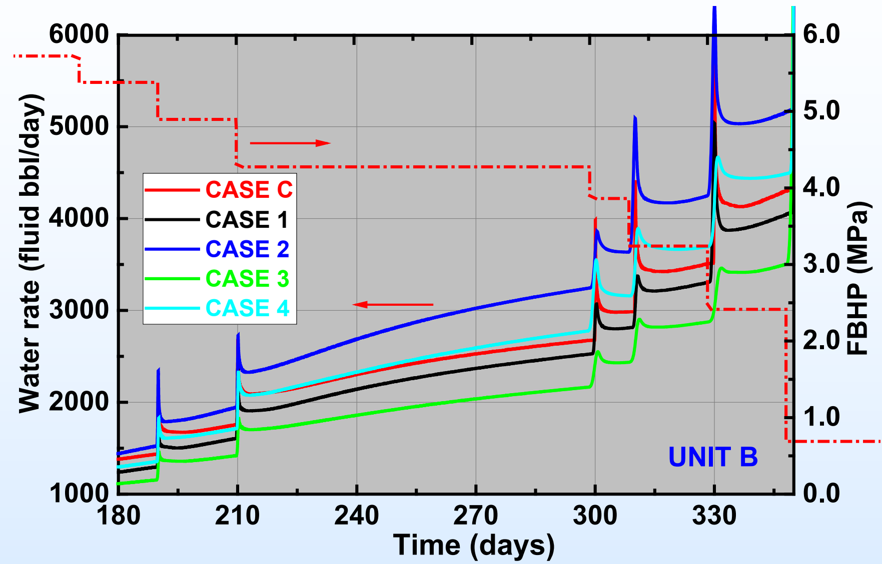

GAS-TO-WATER RATIO

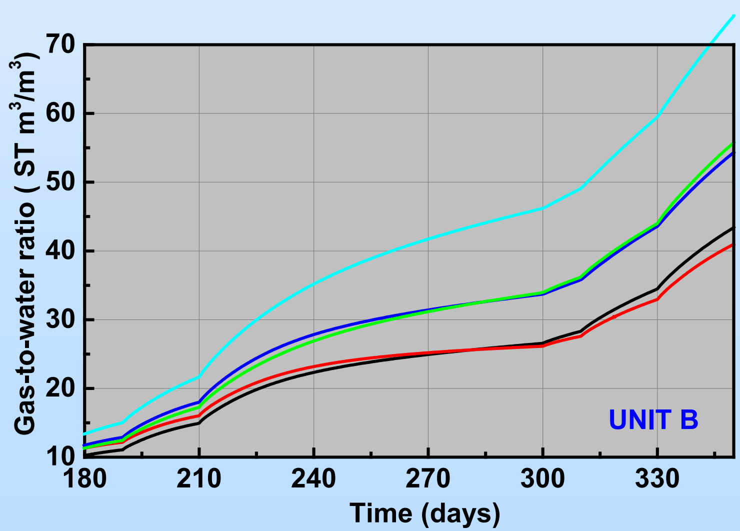

R = 500 m

Scenario 3

Water influx from confining units

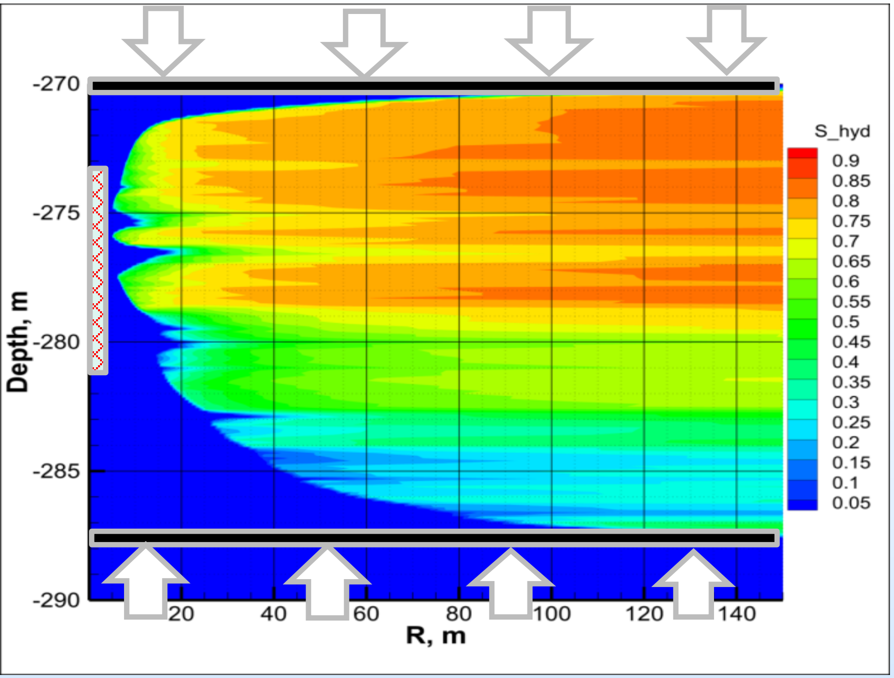

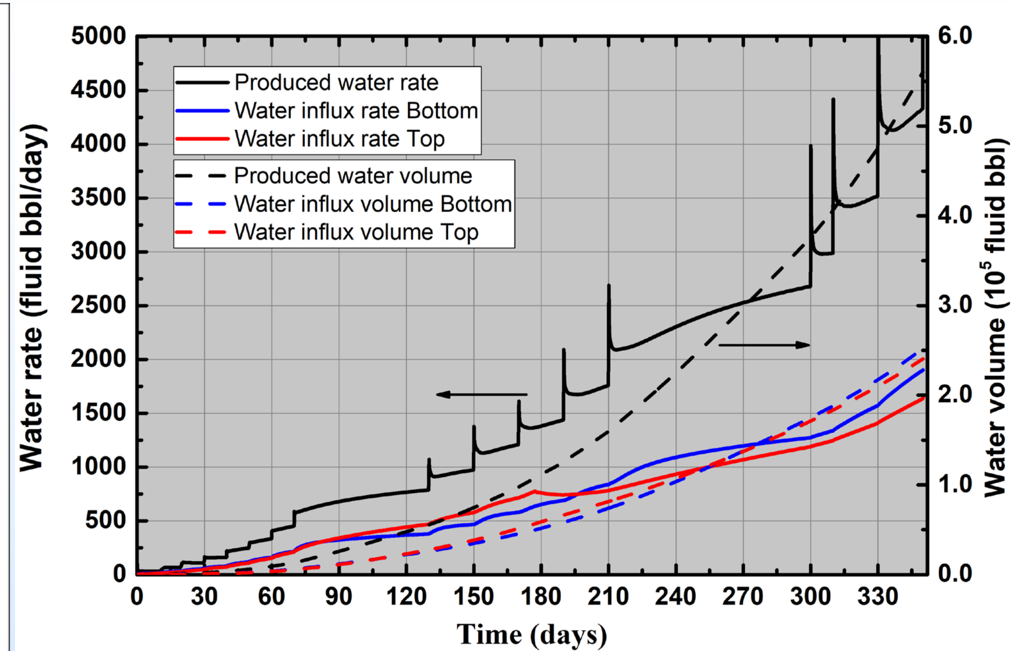

		Day 30		Day 60		Day 90		Day 180		Day 350	
Case	Unit	Gas	Water	Gas	Water	Gas	Water	Gas	Water	Gas	Water
Case C	Res	0.03	1,550	0.13	6,851	0.60	19,547	5.35	83,697	97.12	420,300
	TOP	-	523	-	2,699	-	8,442	-	44,169	-	180,477
	BOT	-	668	-	3,059	-	8,853	-	38,768	-	189,203
Case 1	Res	0.02	1,127	0.10	4,929	0.42	14,567	4.02	69,482	96.42	385,010
	TOP	-	359	-	1,875	-	5,899	-	34,847	-	208,082
	BOT	-	445	-	2,052	-	6,615	-	30,672	-	178,481

Gas (mmscf); Water (bbl)

R = 500 m; Scenario 3

Dissolved gas and released water contributions

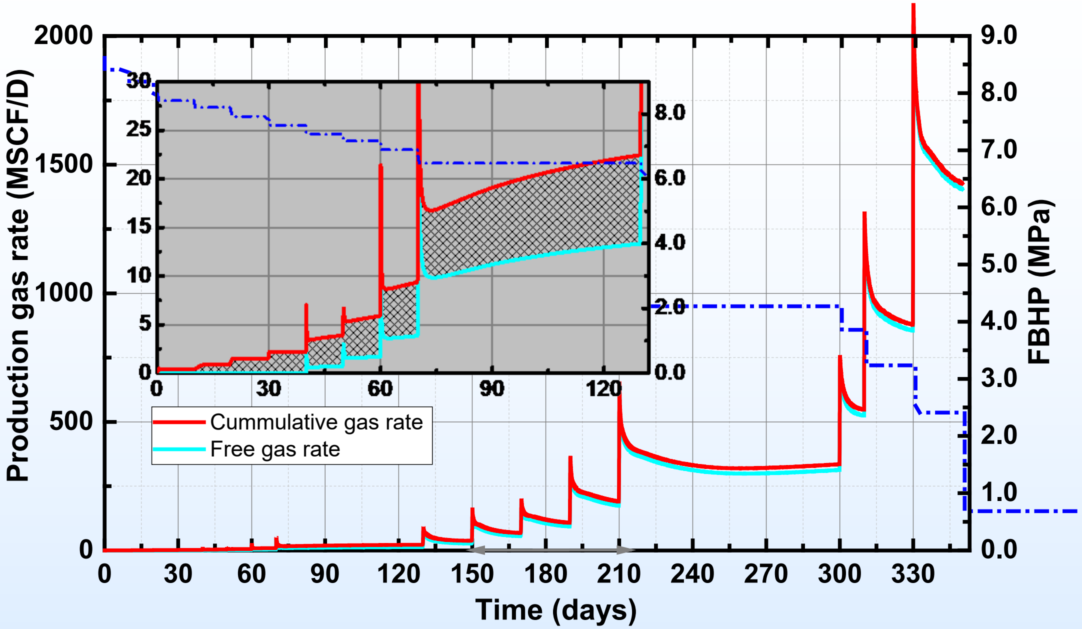

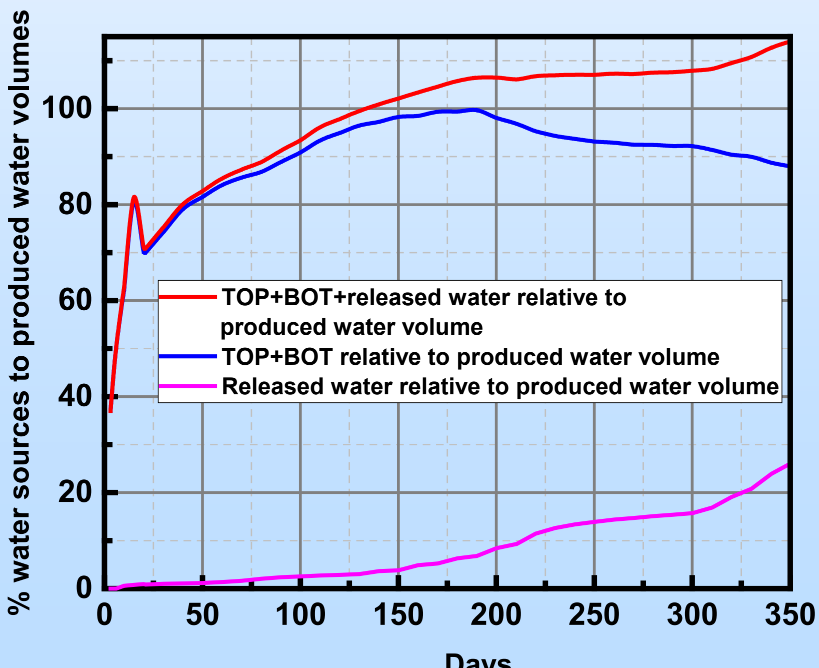

- ✓ Scenario 3 used; R = 500 m.
- ✓ Within first several months more than 50% of produced gas coming as dissolved gas.
- ✓ Contributions from over- and underburden constitutes most of the volume produced.
- ✓ The released water % increase as more gas hydrate dissociates.

Gas hydrate after 1 years of depressurization in B1 sand

CASE C | CASE 1

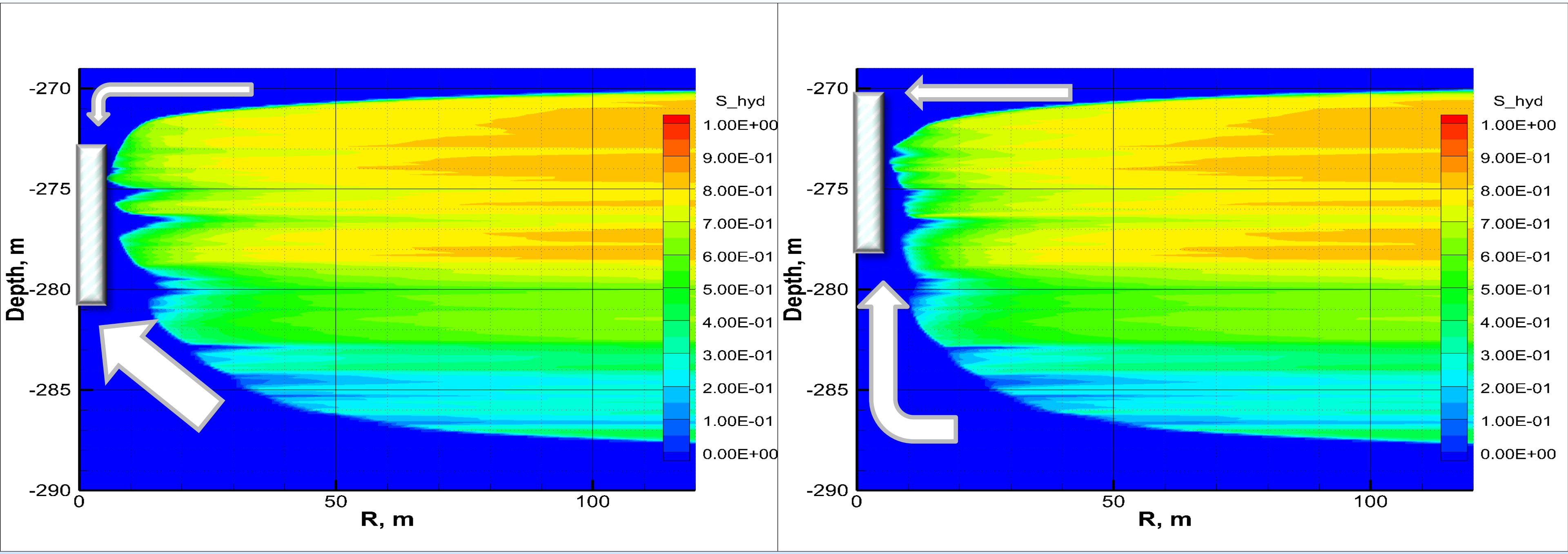

The balance between influxes from over- and underbrden determines overall water production at the wellbore

Summary

- Gas hydrate reservoir in Unit D displays a poor performance compared to that in Unit B due to initial conditions and presence of an underlying aquifer. The gas rates are 0.03 and 1.10 mmscf/day after 1 year of depressurization at 3.0 MPa for the reservoirs in the D1 and B1 sands, respectively with the similar water productivity.

- Water production is dominated by influxes from surrounding strata. Controlling water rates leads to strong decline in gas rates over time.

- Permeability anisotropy, permeability of layers at the top boundary, and placement of a perforated interval are factors impacting productivity.

- Shifting a perforated interval below the top boundary is not necessarily lead to reduced water production. The water productivity is determined by a balance between influxes from over- and underburden.

- Detailed characterization of seal units is mandatory to improve predictions of reservoir performance.

Collaborations & Opportunities

- Collaborations:
  - <u>Reservoir modeling for coupled processes:</u> JOGMEC, LBNL, TAMU, NHU
  - <u>Machine learning application:</u> JOGMEC, USGS, India, Mickey Leland Energy Fellowship
- History-matching predictions of reservoir productivity with field data of brine and gas rates from the ongoing gas hydrate testing at the Kuparuk site, together with a stream of data at monitoring wells recording pressure and temperature changes over a course of depressurization at the production (PTW1) well.
- New Research Area: global climate change impacts, carbon-neutral methane production, industrial applications.

Publications (23-24)

- Myshakin, E., Garapati, N., Chong, L., Seol, Y., Boswell, R. Sensitivity analysis of gas hydrate reservoir (D1 and B1 sands) productivity at the Prudhoe Bay Unit Kuparuk 7-11-12 pad on Alaska North Slope, **2023**, *Prepared.*
- Garapati, N., Myshakin, E. M., Chong, L., Seol, Y., Boswell, R., Haines, S., Collett, T. S. Numerical simulations of depressurization-induced productivity from 3D gas hydrate heterogenous reservoir models (B1 sand) at the Kuparuk 7-11-12 pad on Alaska North Slope, **2023**, *Pending JOGMEC approval.*
- Myshakin, E.M., Chong, L., Seol, Y., NETL Machine Learning Tool Predicts Gas Hydrate Saturation and Occurrence, *Fie in the Ice*, **2023**, 23(1), 1-5.
- Chong, L., Collett, T. S., Creason, C. G., Seol, Y., Myshakin, E. M. Machine Learning Application to Assess Occurrence and Saturations of Gas Hydrate in Marine Sediments Offshore India, *Interpretation*, **2023**, 1-44, https://library.seg.org/doi/10.1190/int-2023-0056.1

- Myshakin, E. M., Garapati, N., Chong, L., Seol, Y., Boswell, R. Numerical simulations of gas hydrate reservoir productivity using 2D and 3D reservoir models of the Prudhoe Bay Unit Kuparuk 7-11-12 pad on the Alaska North Slope, *10th International Conference on Gas Hydrates*, 9-14 July, **2023**, Singapore.